

# Reinforcement Learning for Robust Athletic Intelligence: Lessons from the 2nd “AI Olympics with RealAIGym” Competition

Felix Wiebe<sup>1</sup>, Niccolò Turcato<sup>2</sup>, Alberto Dalla Libera<sup>2</sup>, Jean Seong Bjorn Choe<sup>3</sup>, Bumkyu Choi<sup>3</sup>, Tim Lukas Faust<sup>2</sup>, Habib Maraqten<sup>2</sup>, Erfan Aghadavoodi<sup>1</sup>, Marco Cali<sup>2</sup>, Alberto Sinigaglia<sup>2</sup>, Giulio Giacomuzzo<sup>2</sup>, Diego Romeres<sup>5</sup>, Jong-kook Kim<sup>3</sup>, Gian Antonio Susto<sup>2</sup>, Shubham Vyas<sup>3</sup>, Dennis Mronga<sup>3</sup>, Boris Belousov<sup>4</sup>, Jan Peters<sup>4,6,9,10</sup>, Frank Kirchner<sup>1,7</sup> and Shivesh Kumar<sup>1,8</sup>

**Abstract**—In the field of robotics many different approaches ranging from classical planning over optimal control to reinforcement learning (RL) are developed and borrowed from other fields to achieve reliable control in diverse tasks. In order to get a clear understanding of their individual strengths and weaknesses and their applicability in real world robotic scenarios is it important to benchmark and compare their performances not only in a simulation but also on real hardware. The ‘2nd AI Olympics with RealAIGym’ competition was held at the IROS 2024 conference to contribute to this cause and evaluate different controllers according to their ability to solve a dynamic control problem on an underactuated double pendulum system (Fig. 1) with chaotic dynamics. This paper describes the four different RL methods submitted by the participating teams, presents their performance in the swing-up task on a real double pendulum, measured against various criteria, and discusses their transferability from simulation to real hardware and their robustness to external disturbances.

## I. INTRODUCTION

There are many frameworks for comparing control methods in simulation environments (e.g., [1], [2]) but only few provide a standardized real robot environment which is open and easily reproducible such as [3] with a quadruped robot and [4] with a three end-effector robot for manipulation tasks. The RealAIGym project focuses on simple, low degree of freedom systems capable of dynamic behaviors, such as a simple pendulum [5], AcroMonk [6], RicMonk [7] and the dual purpose double pendulum [8] used in this competition. With the software and hardware being open source and a user friendly Python API, RealAIGym intends to be an open benchmarking platform for comparing control methods on real hardware. This is the 2nd iteration of this competition after the first one having been held at the IJCAI 2023 conference [9].

<sup>1</sup>Robotics Innovation Center, German Research Center for Artificial Intelligence (DFKI), Germany

<sup>2</sup>Department of Information Engineering, University of Padova, Italy

<sup>3</sup>Korea University, Seoul, South Korea

<sup>4</sup>Systems AI for Robot Learning, German Research Center for Artificial Intelligence (DFKI), Germany

<sup>5</sup>Mitsubishi Electric Research Lab (MERL), USA

<sup>6</sup>Technical University of Darmstadt, Germany

<sup>7</sup>University of Bremen, Germany

<sup>8</sup>Chalmers University of Technology, Sweden

<sup>9</sup>Center for Cognitive Science, Germany

<sup>10</sup>Hessian.AI, Germany

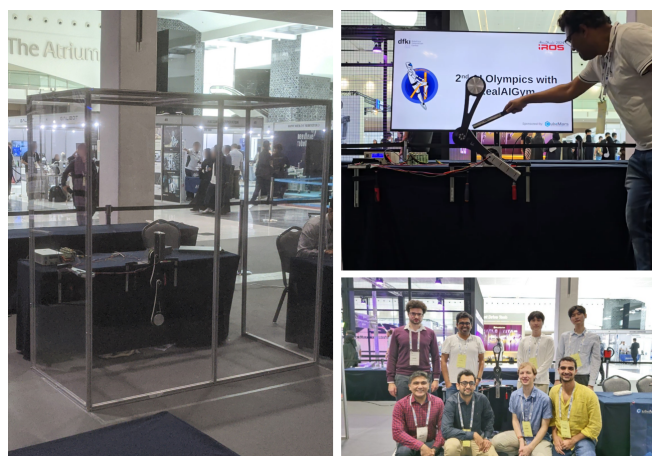


Fig. 1. Onsite setup of the double pendulum hardware (left), the pendulum being disturbed with a stick (top right) and participating teams (bottom right) at IROS 2024.

## II. COMPETITION RULES

The competition was conducted with the dual purpose double pendulum system introduced in [8] which can be operated as an acrobot or pendubot without changing the hardware. For the competition acrobot and pendubot were treated as separate challenges and evaluated in separate tracks. The task on both systems is to swing up the pendulum from the free hanging position to the upright position and stabilize it there. To test the controllers’ robustness, external perturbations are applied on both motors during the execution. The used system had an attached mass of 0.5kg and link lengths of 0.2m and 0.3m. Model parameters identified with least squares optimization were provided to the participants, but the teams were free to do their own system identification.

The competition was carried out in three phases: (i) A simulation phase, (ii) a remote hardware phase and (iii) an onsite phase. In the simulation phase the participants were asked to develop a controller for the swing-up and balance task on the acrobot and/or pendubot system and integrate it into the double pendulum toolkit on github<sup>1</sup>. After the simulation phase, the four best performing controllers were advanced to the next phase. In the remote hardware

<sup>1</sup>[https://github.com/dfki-ric-underactuated-lab/double\\_pendulum](https://github.com/dfki-ric-underactuated-lab/double_pendulum)

phase, the teams got the opportunity to remotely operate the pendulum hardware and collect data from the real system along with live video feed. The third phase took place on site at the IROS 2024 conference, where the teams were able to fine-tune their controllers before the final evaluation.

For the evaluation of the controllers different criteria were considered. Simulation results were evaluated with the *performance score*, where the controllers show their basic functionality. and with the *robustness score*, where the controllers show their robustness to external influences.

The formula for the performance score is:

$$S_p = c_{succ} \left[ 1 - \frac{1}{5} \sum_{i \in \{t, E, \tau_c, \tau_s, v\}} \tanh(w_i c_i) \right] \quad (1)$$

based on the swing-up success  $c_{succ} \in \{0, 1\}$ , the swing-up time  $c_t$ , the used energy  $c_E$ , the torque cost  $c_{\tau_c}$ , the torque smoothness  $c_{\tau_s}$  and the velocity cost  $c_v$ . These quantities are normalized with the weights in Table I and scaled with the  $\tanh$  function to the interval  $[0, 1]$ .

The second score computed from the simulation results is the robustness score:

$$S_r = \frac{1}{6} (c_m + c_{v, \text{noise}} + c_{\tau, \text{noise}} + c_{\tau, \text{resp.}} + c_d + c_p) \quad (2)$$

with the criteria

- Model inaccuracies  $c_m$ : The independent model parameters are varied one at the time in the simulator while using the original model parameters in the controller.
- Measurement noise  $c_{v, \text{noise}}$ : Artificial noise is added to the velocity measurements.
- Torque noise  $c_{\tau, \text{noise}}$ : Artificial noise is added to the motor torque.
- Torque response  $c_{\tau, \text{resp.}}$ : A delayed motor response is modeled by applying the torque  $\tau = \tau_{t-1} + k_{resp}(\tau_{des} - \tau_{t-1})$  instead of the desired torque  $\tau_{des}$ , where,  $\tau_{t-1}$  is the applied motor torque from the last time step and  $k_{resp}$  is the factor which scales the responsiveness.
- Time delay  $c_d$ : A time delay is added to all measurements.
- Random perturbations  $c_p$ : A randomly generated sequence of Gaussian perturbations is added to the applied torque.

For each criterion the severity of the external influence is varied in  $N = 21$  steps (for the model inaccuracies for each independent model parameter) and the score is the percentage of successful swing-ups under these circumstances. For the perturbation criterion 50 random perturbations profiles are generated and evaluated.

For hardware phases, only the performance score,  $S_p$  (1), was calculated with slightly adjusted weights (Table I), but the controllers had to showcase their robustness by reacting to unknown external perturbations during the experiment. The perturbations consist of Gaussian torque profiles on both joints at random times, which were unknown to the controllers. Each trial lasts for 10s and is considered successful if, in the end, the end-effector is at a height above the threshold of 0.45 cm above the base. The teams were

allowed to use up to 0.5Nm torque on the passive joint for friction compensation. Each controller was tested in 10 trials and the final score is the average of the individual scores.

TABLE I  
WEIGHTS FOR THE PERFORMANCE SCORE (1).

	$w_t$	$w_E$	$w_{\tau_c}$	$w_{\tau_s}$	$w_v$
Simulation	$\pi/20$	$\pi/60$	$\pi/20$	$10\pi$	$\pi/400$
Hardware	$\pi/20$	$\pi/60$	$\pi/100$	$\pi/4.0$	$\pi/400$

### III. ALGORITHMS

Four teams advanced to the final round of the competition and tested their control methods on the real hardware. This section briefly introduces the four methods and how they approached the task to improve robustness.

#### A. Model-based RL: MC-PILCO

MC-PILCO (Monte Carlo - Probabilistic Inference for Learning COntrol) [10] is a Model-Based policy gradient RL algorithm. MC-PILCO relies on Gaussian Processes (GPs) to learn the system dynamics from data, and a particle-based policy gradient optimization procedure to update the policy parameters. Let  $\mathbf{x}_t$  and  $\mathbf{u}_t$  be, respectively, the state and input of the system at step  $t$ . A cost function  $c(\mathbf{x}_t)$  encodes the task to solve. A policy  $\pi_{\theta} : \mathbf{x} \rightarrow \mathbf{u}$  parametrized by  $\theta$  selects the inputs applied to the system. The objective is to find the policy parameters  $\theta^*$  which minimize the cumulative expected cost:

$$J(\theta) = \sum_{t=0}^T \mathbb{E}[c(\mathbf{x}_t)] \quad x_0 \sim p(x_0), \quad (3)$$

where  $c(\mathbf{x}_t)$  is a saturated distance as used in [10] and [11].

MC-PILCO iterates attempts to solve the objective task, also called trials. Each trial is composed of three main steps: (i) model learning, (ii) policy update, and (iii) policy execution. Fig. 2 illustrates the main details of each phase.

In the model learning step, previous experience is used to derive a one-step-ahead stochastic system dynamics model, using Gaussian Process Regression. The policy update step aims at minimizing the cost in (3) w.r.t.  $\theta$ . The expectation in (3) is approximated using the GP dynamics derived in step (i) and Monte Carlo particle-based simulation. Finally, in the last step, the new optimized policy is executed on the system and the collected data is stored to update the model in the next trials.

Generally, a well-trained policy can recover if disturbances push the system away from its trajectory. For the sake of the competition, it is preferred to train a policy that can counter these disturbances, without falling and re-maneuvering. To make the policy more robust to these perturbations, we simulate their effects during policy optimization. Namely, for each particle we compute a disturbance profile  $\hat{\mathbf{d}}_t^{(m)}$ ,  $m = 1, \dots, M$ ,  $t = 0, \dots, T$ , using the known disturbance profile distribution. Then, when performing the estimation

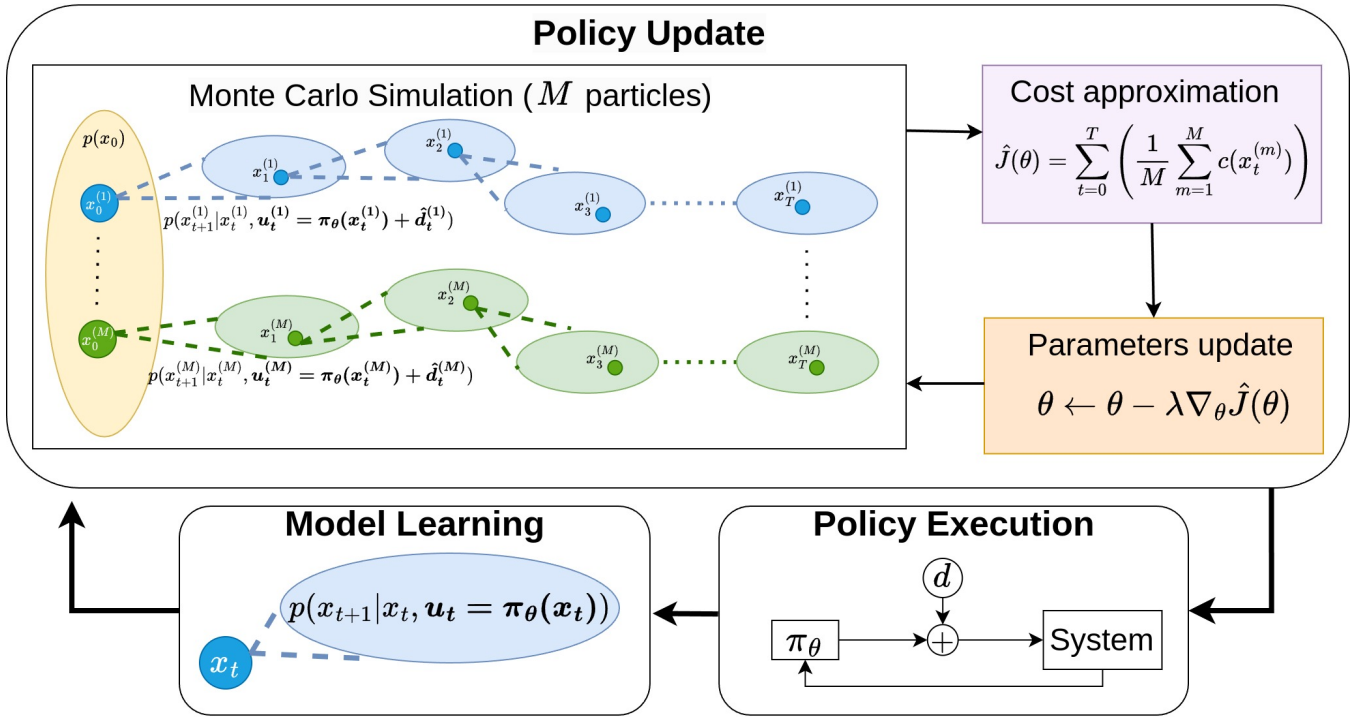


Fig. 2. Schematic representation of the robust MC-PILCO algorithm. Each Episode is composed of (i) model learning, (ii) policy update and (iii) policy execution.

of the forward dynamics in the policy optimization step, the one-step-ahead evolution of the particles is computed as

$$\mathbf{x}_{t+1}^{(m)} = \mathbf{x}_t^{(m)} + \hat{f}(\mathbf{x}_t, \pi_\theta(\mathbf{x}_t^{(m)}) + \hat{\mathbf{d}}_t^{(m)}), \quad (4)$$

where  $\hat{f}(\cdot, \cdot)$  is the forward dynamics model estimated in the model learning phase. The cost function encourages the policy to reject such disturbances while limiting additional maneuvers.

### B. Model-free RL, Average-Reward Entropy Advantage Policy Optimization (AR-EAPO)

Average-Reward Entropy Advantage Policy Optimization (AR-EAPO) is a model-free RL algorithm that extends Entropy Advantage Policy Optimization (EAPO) [12], a maximum entropy (MaxEnt) on-policy actor-critic algorithm, into the average-reward setting.

AR-EAPO tackles the challenge of applying model-free RL to this complex problem by formulating the system as a recurrent Markov Decision Process (MDP), where every state is reachable from every other state in a finite number of steps [13]. With the formulation, instead of using discounted cumulative rewards, AR-EAPO optimizes for long-term average rewards. This approach enables the use of straightforward reward functions aiming for long-term optimality rather than sophisticated reward functions for discounted settings. Here, the proposed solution utilizes a simple quadratic cost function.

Specifically, the objective of AR-EAPO is to optimize the *gain* – the sum of expected average reward and entropy  $\tilde{\rho}^\pi$  for a stationary policy  $\pi$ :

$$\tilde{\rho}^\pi(s) := \lim_{T \rightarrow \infty} \frac{1}{T} \mathbb{E} \left[ \sum_{t=0}^{T-1} r_t - \tau \log \pi(a_t | s_t) \mid s_0 = s, s_t \sim \pi \right], \quad (5)$$

where  $s_t$  is the state of the MDP at time  $t$ ,  $a_t$  is the action at time  $t$ , and  $r_t$  is the reward received at time  $t$ . Building on EAPO's framework, AR-EAPO separately estimates reward and entropy objectives.

Additionally, it incorporates a gain approximation mechanism using advantage estimations [14]:

$$\tilde{\rho}^{k+1} = \tilde{\rho}^k + \eta \mathbb{E}_t[\tilde{A}^\pi(s_t, a_t)], \quad (6)$$

where  $\tilde{\rho}^k$  represents the gain estimate at  $k$ -th iteration,  $\tilde{A}^\pi$  denotes the soft advantage function,  $\eta$  is the step size hyperparameter. The algorithm samples state-action pairs  $(s_t, a_t)$  from rollout trajectories to estimate the advantages using generalized advantage estimation (GAE) [15]. Thus, this formulation effectively extends the well-established proximal policy optimization (PPO) [16] to the average-reward MaxEnt RL setting.

In the double pendulum system, AR-EAPO demonstrates an interesting learning pattern. While the cost objective drives the controller to develop an efficient swing-up policy, the entropy component prevents the pendulum from remaining stationary at the uppermost position (Fig. 3). Instead, it encourages movement toward lower positions where average entropy is higher. Therefore, through these endless swings-ups and downs, the average-reward MaxEnt RL formulation naturally promotes diverse trajectories, thereby achieving a robust control policy.

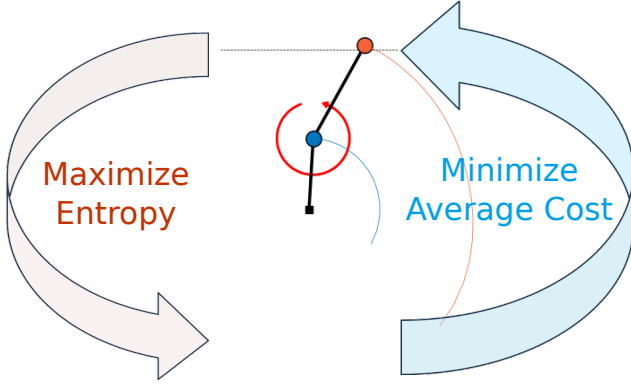


Fig. 3. Illustration of AR-EAPO in the double pendulum system: learning efficient and robust control in an infinite loop of swing-ups while balancing the cost and the entropy.

### C. Model-free RL, Actor-Critic Method: EvolSAC

This section presents the EvolSAC algorithm for the AI Olympics competition. The approach integrates model-free deep RL with evolutionary strategies to optimize control performance in both simulation and real hardware stages. EvolSAC is presented in more detail in [17].

The core algorithm used is Soft Actor-Critic (SAC) [18], a state-of-the-art RL method designed for continuous action spaces. SAC is a model-free RL algorithm that optimizes a stochastic policy by maximizing both the expected reward and the entropy of the policy, which promotes exploration and robustness. SAC’s objective function is defined as:

$$J(\pi) = \mathbb{E}_{s_t, a_t \sim \pi} \left[ \sum_t \gamma^t (r(s_t, a_t) + \alpha \mathcal{H}(\pi(\cdot | s_t))) \right],$$

where  $\gamma$  is the discount factor,  $r(s_t, a_t)$  is the reward function,  $\alpha$  is a temperature parameter that weighs the importance of the entropy term  $\mathcal{H}$ , encouraging the policy to explore a wide range of actions.

The initial stage of the methodology involves training the SAC agent with a physics-inspired surrogate reward function. This function is designed to approximate the complex objectives of the competition, which includes factors like swing-up success, energy consumption, and torque smoothness. The surrogate reward function aims to guide the agent towards achieving the swing-up task while managing the energy costs effectively:

$$R(s, a) = \begin{cases} V + \alpha[1 + \cos(\theta_2)]^2 - \beta T & \text{if } y > y_{th} \\ -\rho_1 a^2 - \phi_1 \Delta a & \\ V - \rho_2 a^2 - \phi_2 \Delta a - \eta \|\dot{s}\|^2 & \text{otherwise} \end{cases} \quad (7)$$

where  $\alpha, \beta, \phi, \eta, \rho$  are hyperparameters used to control the trade-offs.

To address the challenge of optimizing a policy for both performance and robustness, the methodology incorporates evolutionary strategies in the later stages of training. Evolutionary strategies are gradient-free optimization methods that are particularly effective in scenarios where the landscape of the objective function is rugged or noisy. One specific

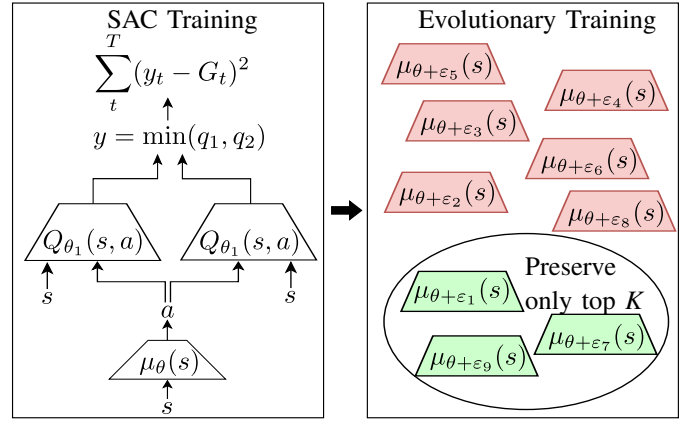


Fig. 4. Summary of training for EvolSAC. Left: SAC training for optimal policy, right: Evolutionary selection of high scoring and robust policies.

strategy used is the Separable Natural Evolution Strategy (SNES) [19], which updates mutation strengths using a log-normal distribution, allowing efficient exploration of the parameter space:

$$\begin{bmatrix} \sigma_{\text{new}, i} \\ \theta_{\text{new}, i} \end{bmatrix} = \begin{bmatrix} \sigma_{\text{old}, i} \exp(\tau \mathcal{N}(0, 1) + \tau' \mathcal{N}(0, 1)_i) \\ \theta_{\text{old}, i} + \sigma_{\text{new}, i} \mathcal{N}(0, 1)_i \end{bmatrix} \quad (8)$$

where  $\tau, \tau'$  are learning rates controlling the mutation rate.

SNES is used to fine-tune the policy obtained from SAC, directly optimizing against the competition’s score function defined in (1). This two-step process, initial training with SAC followed by fine-tuning with SNES, ensures that the developed controller is not only effective in achieving the desired task but also robust against various disturbances and model inaccuracies. The overall training strategy is illustrated in Fig. 4.

### D. Model-free RL, Actor-Critic Method: HistorySAC

This section proposes a solution for the challenge that combines the Soft Actor-Critic algorithm with a method for learning temporal features. The intuition behind this method is that it is not possible to infer system parameters, such as the masses of both links, from a single state. This method aims to implicitly encode the system dynamics by extracting temporal features with convolutional and linear layers from previous measurements. For this, the velocities of eleven previous and the current time step are encoded in a learned temporal context and this context is concatenated with the current state before feeding it into the actor and critic networks (Fig. 5). The temporal information is encoded by using two 1-dimensional convolutional layers with a kernel size of five and an output size of twelve, followed by two linear layers with a width of 256, where the first uses a ReLU and the second uses a tanh activation function. The underlying reinforcement learning algorithm is the Stable-Baselines3 implementation of SAC [1], but with a layer size of 1024 instead of the original 256 for the fully-connected layers. It is important to note that the networks of actor and critic do not share parameters.



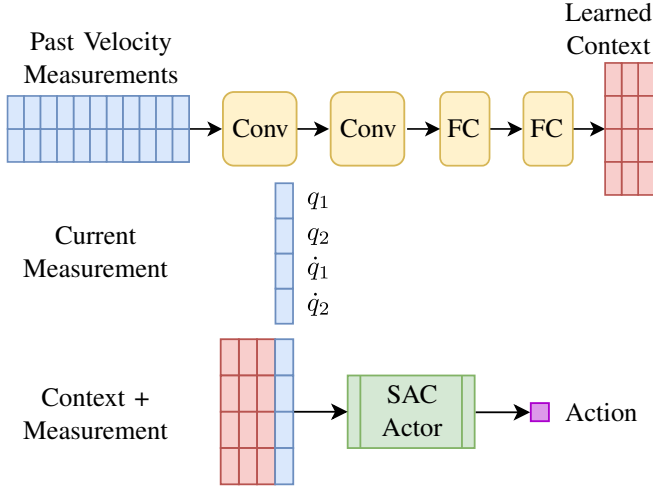


Fig. 5. The model architecture for encoding the history into a context representation in HistorySAC. A sequence of past velocity measurements is passed through convolutional (Conv) and fully-connected (FC) layers, and the output is attached to the current measurement before being passed to the actor and critic in SAC.

The training uses the reward function

$$R_2(s, a) = -0.05 \cdot \left( (q_1 - \pi)^2 + q_2^2 \right) - \left[ 0.02 \cdot \left( \dot{q}_1^2 + \dot{q}_2^2 \right) + 0.25 \cdot \left( a^2 + 2|a| \right) + 0.02 \cdot \left| \frac{a - a_{\text{prev}}}{dt} \right| + 0.05 \cdot (\dot{q}_i \cdot a) \right], \quad (9)$$

with the state  $s$  being the angles of both joints  $q_1$  and  $q_2$ , and their derivatives. A regularization term (squared brackets) is subtracted which includes the angular velocities, the agent's action  $a$  and the previous action  $a_{\text{prev}}$ . For pendubot,  $\beta$  was set to  $\beta = 0.1$  and  $\dot{q}_i = \dot{q}_1$  and for acrobot  $\beta = 0.025$  and  $\dot{q}_i = \dot{q}_2$ . In this application it turned out that providing the agent with negative values (punishments) instead of positive values (rewards) leads to better performance and higher robustness. Having the highest possible value of the reward function at 0 makes learning the Q-function much more stable than having an optimal value that is positive, since a successful swing-up policy does not suddenly change the Q-values of all previous states and thus prevents policy degradation after learning successful swing-ups.

Successful swing-up attempts on the real system using a policy that was purely trained in simulation require an accurate identification of the physical parameters of the double pendulum model. Differential Evolution [20], which is a gradient-free optimization algorithm, was used to optimize for the physical parameters of the simulated double pendulum  $\theta_m$  to minimize the sim-to-real gap. The cost function for the optimization was chosen to be an importance-weighted squared error between simulated and

real trajectories:

$$J(\theta_m) = \sum_{i=1}^{N_{\text{traj}}} \sum_{t=1}^{T_i} \sum_{j=1}^m \left( 1 - \frac{0.5(t-1)}{T_i-1} \right) \times \left( x_{\text{sim},j}^{(i)}[t; \theta_m] - x_{\text{real},j}^{(i)}[t] \right)^2. \quad (10)$$

Here  $m = 4$  the number of state indices,  $T_i$  is the time steps in a trajectory, and  $N_{\text{traj}}$  the number of trajectories.

Data from the real system was collected using swing-up policies that were trained in simulation for acrobot and pendubot. The torque time series from these trajectories is then used to create trajectories on the simulated system, resulting in pairs of trajectories for a single torque curve,  $x_{1:T}^{\text{real}}$  and  $x_{1:T}^{\text{sim}}$ . The first round brackets in (10) denote a time-dependent weight. The weighting decreases linearly over the trimmed trajectory from 1 to 0.5, so that later points in the trajectory with a larger error accumulation have less impact. Since a solution for the optimization problem becomes increasingly hard to find with a longer trajectory, only the first 1.5 seconds of each trajectory are considered in the optimization.

For the training process, a multi-environment strategy, incorporating multiple solutions of the previous system identification process, prevented overfitting on a single environment.

## IV. RESULTS

The computed scoring criteria and final scores for all controllers are visualized in Fig. 6. Data, figures and videos of the individual attempts can be found on the online leaderboards<sup>2</sup>. The accompanying video of this paper shows the swing-ups in simulation and on the real hardware as well as the controllers robustness to disturbances induced by hitting the pendulum with a stick.

### A. Acrobot

In the simulation phase HistorySAC and AR-EAPO showed the best performances (0.66 and 0.63) with a fast swing-up below 1 s, little and smooth torque usage and low velocities. They also showed good robustness results (0.75 and 0.73) especially concerning robustness to torque noise, torque responsiveness and delay. Like all other controllers, they were most sensitive to velocity noise. EvolSAC showed convincing results as well (perf. 0.52, robust. 0.69) only slightly behind HistorySAC and AR-EAPO. MC-PILCO was the least efficient controller of these four (perf. 0.31), with a higher energy usage and a less smooth torque signal. In the robustness score MC-PILCO was very sensitive in all criteria except for torque responsiveness and perturbations (robust. 0.24). In the hardware phase, the model based algorithm MC-PILCO was trained based on recorded data from the real system which resulted in a policy which captured knowledge about effects which are not considered in the simple mathematical model. The policy proved to be very robust to the unknown external perturbations and MC-PILCO

<sup>2</sup>[https://dfki-ric-underactuated-lab.github.io/real-ai-gym\\_leaderboard/](https://dfki-ric-underactuated-lab.github.io/real-ai-gym_leaderboard/)

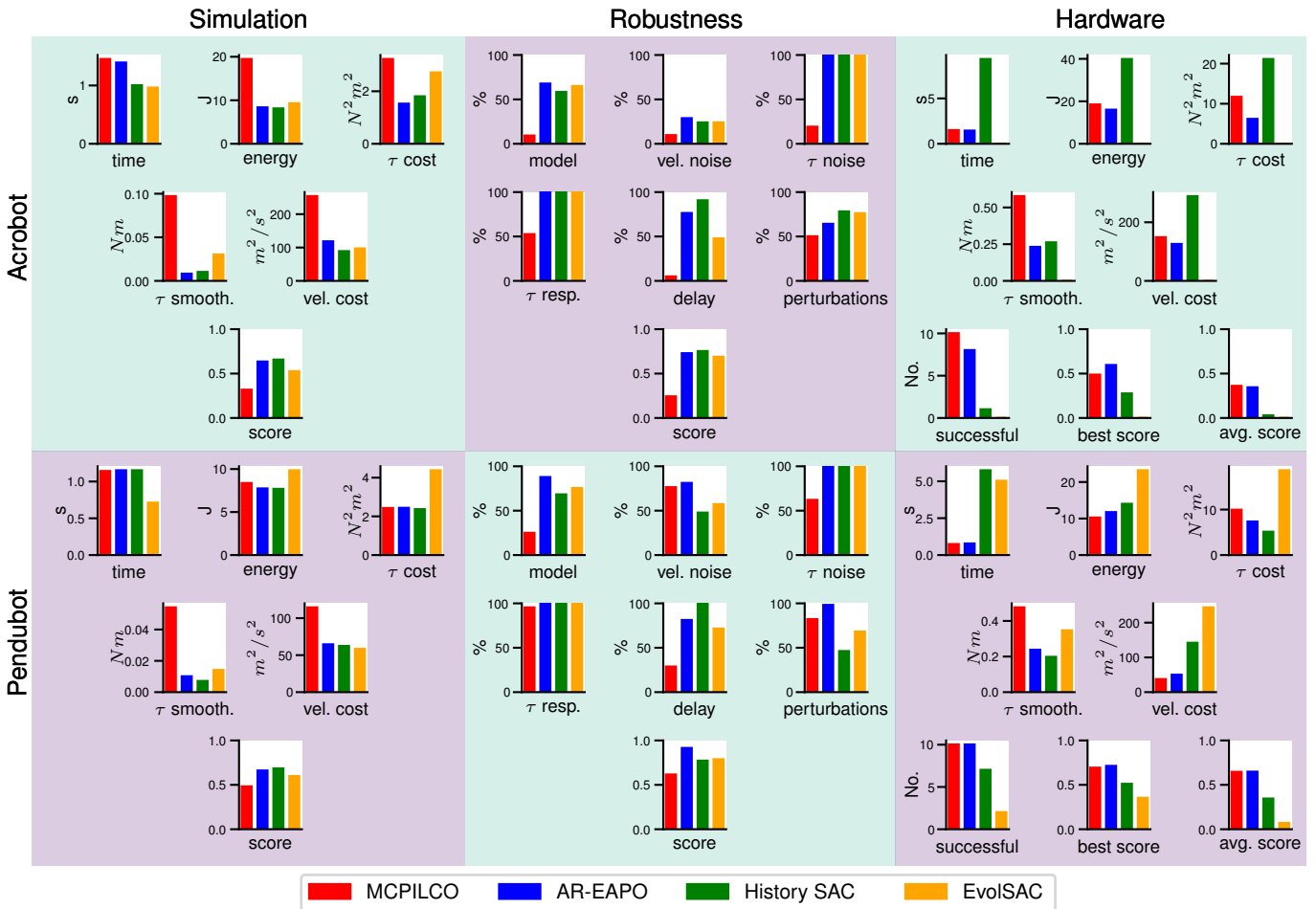


Fig. 6. All scores of the final round controllers. The simulation and robustness columns are computed from simulation data while the hardware score is evaluated from experiments on the real system. Note that for the simulation and hardware criteria lower values are better while for the success scores in the robustness tests higher values are better. For the final scores 1.0 is the best achievable rating.

achieved 10/10 successful swing-ups (hardware avg. score 0.36). The swing-up trajectory of the highest scoring attempt is shown in Fig. 7. AR-EAPO achieved even better scores in all five criteria but only managed 8/10 successful swing-ups resulting in a better best trial but a very close second place in the average score (avg. score 0.34). HistorySAC achieved only 1/10 swing-ups in the final evaluation (avg. score 0.03) and for EvolSAC the simulation-reality gap was too significant to swing-up the real acrobot system (avg. score 0.00).

### B. Pendubot

On the pendubot, all four controllers showed similar performances in swing-up time and energy usage. EvolSAC is the only one with a significantly higher torque cost and MC-PILCO the only one with a significantly higher torque smoothness value and velocity cost. This results in similar performance scores (HistorySAC: 0.68, AR-EAPO: 0.66, EvolSAC: 0.60, MC-PILCO: 0.48). In the robustness metrics, MC-PILCO again was sensitive to modeling errors and delay. AR-EAPO was quite robust to modeling errors and also very robust (100% success) to random perturbations.

This resulted in good robustness scores for all controllers (AR-EAPO: 0.91, EvolSAC: 0.79, HistorySAC: 0.77, MC-PILCO: 0.61) and AR-EAPO winning this category. On the real hardware, MC-PILCO and AR-EAPO showed very convincing performances with 10/10 successful swing-ups and good scores in the individual criteria. Here, AR-EAPO took the win with a very slight margin (AR-EAPO: 0.65, MC-PILCO: 0.64). The best AR-EAPO trial is shown in Fig. 8. HistorySAC also showed respectable results with 7/10 swing-ups (avg. score: 0.34). The EvolSAC team was not able to attend the conference and thus did not fine-tune the controller for the onsite setup, but EvolSAC was still successful 2/10 times (avg. score: 0.07).

## V. CONCLUSION

The '2nd AI Olympics with RealAIGym' competition at the IROS 2024 conference gives interesting insights into the usability of state of the art RL algorithms on a real robotic system. The fact that all four teams which advanced to the final round submitted RL controllers reflects that RL is a very active research field in robotics. The model based RL method MC-PILCO achieved very good results with a high

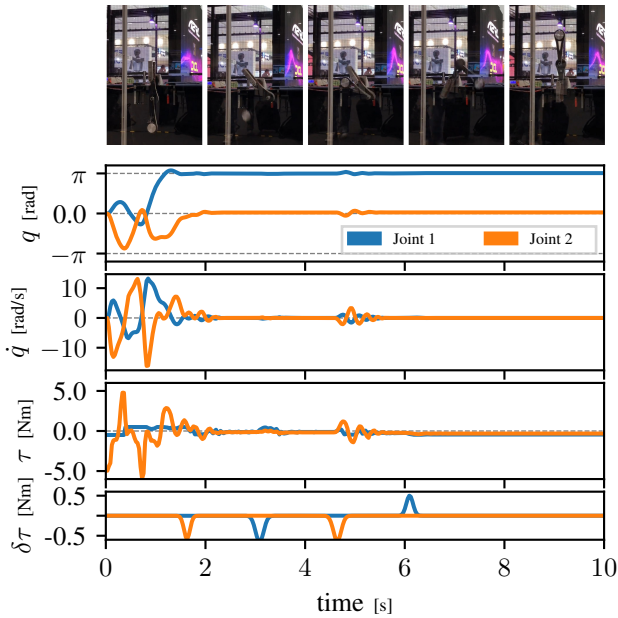


Fig. 7. Swing-up trajectory with MC-PILCO on the real acrobot system. From top to bottom, the plot shows the evolution of the joint angles, velocities, motor torques and disturbances.

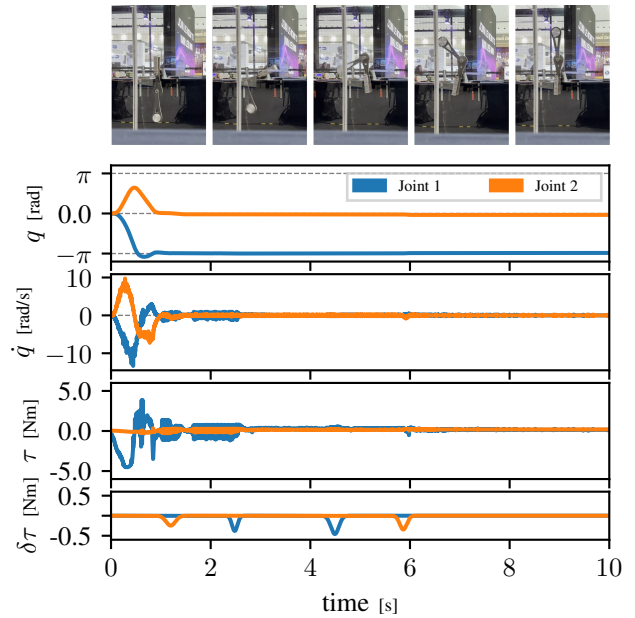


Fig. 8. Swing-up trajectory with AR-EAPO on the real pendubot system. From top to bottom, the plot shows the evolution of the joint angles, velocities, motor torques and disturbances.

robustness by learning very sample efficiently from data recorded from the real system and won the acrobot competition track. The other method which stood out was AR-EAPO, with good scores on both systems and winning the pendubot category. Both methods exhibited a high robustness to unknown perturbations and even recovered most of the time after being pushed far away from their nominal path with a stick, proving to be promising candidates for finding a global swing-up and balance policy for the underactuated double pendulum systems.

We made sure to make all results online available and hope that this competition inspires further research and thorough comparisons of control methods for dynamic behaviors on underactuated robots with high robustness.

## ACKNOWLEDGMENT

The competition organizers at DFKI-RIC (FW, SV, DM, FK, SK) acknowledge the support of M-RoCK project funded by the German Aerospace Center (DLR) with federal funds (Grant Number: FKZ 01IW21002) from the Federal Ministry of Education and Research (BMBF) and is additionally supported with project funds from the federal state of Bremen for setting up the Underactuated Robotics Lab (Grant Number: 201-342-04-1/2023-4-1). TV, BB, and JP acknowledge the grant “Einrichtung eines Labors des Deutschen Forschungszentrum für Künstliche Intelligenz (DFKI) an der Technischen Universität Darmstadt” of the Hessisches Ministerium für Wissenschaft und Kunst. This research was supported by Research Clusters “The Adaptive Mind” and “Third Wave of AI”, funded by the Excellence Program of the Hessian Ministry of Higher Education, Science, Research and the Arts. Parts of the calculations

for this research were conducted on the Lichtenberg high-performance computer of the TU Darmstadt. Alberto Dalla Libera and Giulio Giacomuzzo were supported by PNRR research activities of the consortium iNEST (Interconnected North-Est Innovation Ecosystem) funded by the European Union Next GenerationEU (Piano Nazionale di Ripresa e Resilienza (PNRR) – Missione 4 Componente 2, Investimento 1.5 – D.D. 1058 23/06/2022, ECS\_00000043). This manuscript reflects only the Authors’ views and opinions, neither the European Union nor the European Commission can be considered responsible for them. TV and BB also thank Daniel Palenicek and Tim Schneider for their support while performing the experiments on the IAS group’s computing cluster at TU Darmstadt.

## REFERENCES

- [1] A. Raffin, A. Hill, A. Gleave, A. Kanervisto, M. Ernestus, and N. Dormann, “Stable-baselines3: Reliable reinforcement learning implementations,” *Journal of Machine Learning Research*, vol. 22, no. 268, pp. 1–8, 2021. [Online]. Available: <http://jmlr.org/papers/v22/20-1364.html>
- [2] S. James, Z. Ma, D. R. Arrojo, and A. J. Davison, “Rlbench: The robot learning benchmark & learning environment,” *IEEE Robotics and Automation Letters*, vol. 5, no. 2, pp. 3019–3026, 2020.
- [3] F. Grimmering, A. Meduri, M. Khadiv, J. Viereck, M. Wüthrich, M. Naveau, V. Berenz, S. Heim, F. Widmaier, T. Flayols, J. Fiene, A. Badri-Spröwitz, and L. Righetti, “An open torque-controlled modular robot architecture for legged locomotion research,” *IEEE Robotics and Automation Letters*, vol. 5, no. 2, pp. 3650–3657, 2020.
- [4] N. Funk, C. Schaff, R. Madan, T. Yoneda, J. U. De Jesus, J. Watson, E. K. Gordon, F. Widmaier, S. Bauer, S. S. Srinivasa, T. Bhattacharjee, M. R. Walter, and J. Peters, “Benchmarking structured policies and policy optimization for real-world dexterous object manipulation,” *IEEE Robotics and Automation Letters*, vol. 7, no. 1, pp. 478–485, 2022.
- [5] F. Wiebe, J. Babel, S. Kumar, S. Vyas, D. Harnack, M. Boukheddimi, M. Popescu, and F. Kirchner, “Torque-limited simple pendulum: A toolkit for getting familiar with control algorithms in underactuated

- robotics,” *Journal of Open Source Software*, vol. 7, no. 74, p. 3884, 2022. [Online]. Available: <https://doi.org/10.21105/joss.03884>
- [6] M. Javadi, D. Harnack, P. Stocco, S. Kumar, S. Vyas, D. Pizzutilo, and F. Kirchner, “Acromonk: A minimalist underactuated brachiating robot,” *IEEE Robotics and Automation Letters*, vol. 8, no. 6, pp. 3637–3644, 2023.
- [7] S. S. Grama, M. Javadi, S. Kumar, H. Z. Boroujeni, and F. Kirchner, “Ricmonk: A three-link brachiation robot with passive grippers for energy-efficient brachiation,” in *2024 IEEE International Conference on Robotics and Automation (ICRA)*, 2024, pp. 8920–8926.
- [8] F. Wiebe, S. Kumar, L. J. Shala, S. Vyas, M. Javadi, and F. Kirchner, “Open source dual-purpose acrobot and pendubot platform: Benchmarking control algorithms for underactuated robotics,” *IEEE Robotics & Automation Magazine*, vol. 31, no. 2, pp. 113–124, 2024.
- [9] F. Wiebe, N. Turcato, A. Dalla Libera, C. Zhang, T. Vincent, S. Vyas, G. Giacomuzzo, R. Carli, D. Romeres, A. Sathuluri, M. Zimmermann, B. Belousov, J. Peters, F. Kirchner, and S. Kumar, “Reinforcement learning for athletic intelligence: Lessons from the 1st “ai olympics with realigym” competition,” in *Proceedings of the Thirty-Third International Joint Conference on Artificial Intelligence, IJCAI-24*, K. Larson, Ed. International Joint Conferences on Artificial Intelligence Organization, 8 2024, pp. 8833–8837, demo Track. [Online]. Available: <https://doi.org/10.24963/ijcai.2024/1043>
- [10] F. Amadio, A. Dalla Libera, R. Antonello, D. Nikovski, R. Carli, and D. Romeres, “Model-based policy search using monte carlo gradient estimation with real systems application,” *IEEE Transactions on Robotics*, vol. 38, no. 6, pp. 3879–3898, 2022.
- [11] N. Turcato, A. Dalla Libera, G. Giacomuzzo, R. Carli, *et al.*, “Teaching a robot to toss arbitrary objects with model-based reinforcement learning,” in *2023 9th International Conference on Control, Decision and Information Technologies (CoDIT)*. IEEE, 2023, pp. 1126–1131.
- [12] J. S. B. Choe and J.-K. Kim, “Maximum entropy on-policy actor-critic via entropy advantage estimation,” 2024. [Online]. Available: <https://arxiv.org/abs/2407.18143>
- [13] M. L. Puterman, *Markov decision processes: discrete stochastic dynamic programming*. John Wiley & Sons, 2014.
- [14] V. Dewanto, G. Dunn, A. Eshragh, M. Gallagher, and F. Roosta, “Average-reward model-free reinforcement learning: a systematic review and literature mapping,” *arXiv preprint arXiv:2010.08920*, 2020.
- [15] J. Schulman, P. Moritz, S. Levine, M. Jordan, and P. Abbeel, “High-dimensional continuous control using generalized advantage estimation,” *arXiv preprint arXiv:1506.02438*, 2015.
- [16] J. Schulman, F. Wolski, P. Dhariwal, A. Radford, and O. Klimov, “Proximal policy optimization algorithms,” *arXiv preprint arXiv:1707.06347*, 2017.
- [17] M. Cali, A. Sinigaglia, N. Turcato, R. Carli, and G. A. Susto, “Ai olympics challenge with evolutionary soft actor critic,” *arXiv preprint arXiv:2409.01104*, 2024.
- [18] T. Haarnoja, A. Zhou, P. Abbeel, and S. Levine, “Soft actor-critic: Off-policy maximum entropy deep reinforcement learning with a stochastic actor,” in *International conference on machine learning*. PMLR, 2018, pp. 1861–1870.
- [19] T. Schaul, T. Glasmachers, and J. Schmidhuber, “High dimensions and heavy tails for natural evolution strategies,” in *Proceedings of the 13th annual conference on Genetic and evolutionary computation*, 2011, pp. 845–852.
- [20] R. Storn and K. Price, “Differential evolution—a simple and efficient heuristic for global optimization over continuous spaces,” *Journal of global optimization*, vol. 11, pp. 341–359, 1997.